

## LITERATURE CITED

1. A. F. Aleksandrov, "The impedance of a planar capacitor fully or partially occupied by a plasma," *Zh. Tekh. Fiz.*, 35, No. 2 (1965).
2. F. W. Crawford and R. Grard, "Low-frequency impedance characteristics of a Langmuir probe in a plasma," *J. Appl. Phys.*, 37, No. 1 (1966).
3. V. I. Molotkov and A. P. Poberezhskii, "Investigation of near-wall and near-electrode phenomena by the plasma capacitor method," in: *Low-Temperature Plasma Diagnostics* [in Russian], Nauka, Moscow (1979).
4. H. K. Messerle, M. Sakuntala, and D. Trung, "Arc transition in an MHD generator," *J. Phys. D: Appl. Phys.*, 3, 1080 (1970).
5. B. M. Oliver and R. M. Clements, "Resonance behavior of the ion sheath capacitance near the plasma ion frequency," *J. Appl. Phys.*, 44, No. 3 (1973).
6. E. P. Velikhov, V. S. Golubev, and V. V. Chernukha, "Possibility of MHD transformation of the energy of pulsed thermonuclear reactors," *At. Energ.*, 36, No. 4 (1974).
7. V. G. Pikulin, "A pulse circuit for measuring small capacitance of capacitors with losses," *Izmer. Tekh.*, No. 3 (1972).
8. E. K. Chekalin and L. V. Chernykh, "Electrostatic wall probe in low-temperature plasma flow," *Zh. Prikl. Mekh. Tekh. Fiz.*, No. 1 (1981).

## NUMERICAL STUDY OF A GLOW DISCHARGE IN

A CO<sub>2</sub>-N<sub>2</sub>-He GAS MIXTURE

R. S. Galeev and R. T. Faizrahmanov

UDC 537.521

Increased interest has developed in the volume glow discharge in CO<sub>2</sub>-N<sub>2</sub>-He gas mixtures because of their wide use as active media in gas discharge lasers. The presence of intense dissipative electron attachment in electronegative gases (among which is the CO<sub>2</sub>-N<sub>2</sub>-He mixture) has a strong effect on the structure and evolution of the glow discharge. Thus, under certain conditions, attachment instability develops in the discharge [1, 2], while in the stable state the positive column of the discharge may be inhomogeneous along the direction of the current [2, 3].

Attachment instability was analyzed in the linear approximation in [4, 5] with the assumption of homogeneity of the discharge positive column. A qualitative study of the structure of domains which develop with attachment instability was performed in [6-9]. Numerical calculations of evolution of a volume glow discharge in an electronegative gas were presented in [10-12].

When the non-steady-state equations describing such a discharge are integrated [10, 11], a complete physical picture of discharge evolution can be obtained. The total time required for exit of the solution to steady-state (or steady-state oscillations) is determined by the slowest process (ion drift). The more rapid drift of electrons imposes rigid limitations on the integration step used for time. Therefore it is clear that use of the established method to obtain the steady-state solution will require significant expenditures of machine time.

To obtain the steady-state solution the present study employs an effective method for solution of the steady-state problem, allowing study of volume glow discharges over a wide range of parameters and construction of current-voltage characteristics (CVCs) for the discharge. In calculating discharges in the attachment instability region the nonsteady-state equations were integrated numerically using an implicit difference method.

1. Mathematical Model and Methods of Solution. Within the framework of the assumptions generally used [1, 2], the nonsteady-state equations describing a volume glow discharge in an electronegative gas have the following form:

---

Kazan'. Translated from *Zhurnal Prikladnoi Mekhaniki i Tekhnicheskoi Fiziki*, No. 5, pp. 5-10, September-October, 1987. Original article submitted June 4, 1986.

$$\begin{aligned}
\frac{\partial q_e}{\partial t} + \frac{\partial j_e}{\partial x} &= (\nu_i - \nu_a) q_e - \frac{\beta_e}{e} q_e q_+ - k_d N q_- + Q, \\
\frac{\partial q_+}{\partial t} - \frac{\partial j_+}{\partial x} &= \nu_i q_e - \frac{\beta_e}{e} q_e q_+ - \frac{\beta_i}{e} q_+ q_- + Q, \\
\frac{\partial q_-}{\partial t} + \frac{\partial j_-}{\partial x} &= \nu_a q_e - \frac{\beta_i}{e} q_+ q_- - k_d N q_-, \quad \frac{\partial E}{\partial x} = 4\pi (q_e + q_- - q_+), \\
j_k &= V_k q_k, \quad V_k = \mu_k E. \quad q_k = en_k \quad (k = e, +, -).
\end{aligned} \tag{1.1}$$

Here  $n_k$  is the charged particle concentration;  $q_k$ , the charge density;  $j_k$ , current density;  $V_k$ , drift velocities;  $\mu_k$ , mobilities (the subscripts  $e$ ,  $+$ ,  $-$  refer to electrons, positive and negative ions, respectively);  $E$  is the electric field intensity;  $\nu_i = \nu_i(E/N)$ ,  $\nu_a = \nu_a(E/N)$  are the shock ionization and dissociative attachment frequencies;  $k_d$ ,  $\beta_e$ ,  $\beta_i$  are detachment, electron-ion, and ion-ion recombination coefficients;  $Q$  is the rate of electron pair generation by the external ionization source;  $e$  is the charge of the electron;  $N$  is the total number of gas molecules per unit volume.

The field intensity satisfies the condition

$$\int_0^L E(x, t) dx = U \tag{1.2}$$

(where  $U$  is the potential difference between the electrodes).

At the cathode ( $x = 0$ ) and anode ( $x = L$ ) the expressions

$$j_e(0, t) = \gamma j_+(0, t), \quad j_-(0, t) = j_+(L, t) = 0 \tag{1.3}$$

are satisfied, where  $\gamma$  is the coefficient of secondary electron emission from the cathode upon ion bombardment. Nonsteady-state problem (1.1)-(1.3) will be solved for initial conditions  $q_e(x, 0) = q_+(x, 0) = q_0 \equiv \text{const}$ ,  $q_-(x, 0) = 0$ .

The charge transport equations are approximated by an implicit difference scheme of the "traveling count" type [13]

$$\frac{1}{\tau} (q_i^{m+1} - q_i^m) + \frac{1}{2h} [(q_i^{m+1} + q_i^m) V_i^{m+1} - (q_{i-1}^{m+1} + q_{i-1}^m) V_{i-1}^{m+1}] = \frac{1}{4} (f_i^m + f_{i-1}^m + f_i^{m+1} + f_{i-1}^{m+1}). \tag{1.4}$$

Here  $\tau$  and  $h$  are the steps in time and space; the subscripts  $i$  and  $m$  enumerate nodes along  $x$  and  $t$ ;  $f$  is the right side of the transport equation.

To define the electric-field intensity we use the equation of conservation of current density [14], which in combination with the implicit scheme of Eq. (1.4) allows an increase in the time integration step for system (1.1) by two orders of magnitude, as compared to explicit schemes.

For the case of a steady-state discharge there follows from system (1.1) the existence of a total current integral

$$j_e + j_+ + j_- = j \equiv \text{const}. \tag{1.5}$$

The total current density  $j$  is assumed a specified value while the voltage across the electrodes  $U$  is found from Eq. (1.2).

Equation (1.5) allows elimination of, for example,  $j_-$  from system (1.1), reducing the order of the system by unity. To integrate the system of three differential equations with boundary conditions (1.3) thus obtained we use the Newton-Kantorovich successive approximation method [15]. The essence of this method for the problem under consideration is as follows. We write the system in vector notation in the form

$$\frac{dz}{dx} = \mathbf{F}(z), \quad z = \begin{pmatrix} j_e \\ j_+ \\ E \end{pmatrix} \tag{1.6}$$

(where  $z$  is the vector of the unknowns;  $\mathbf{F}$  the vector of the right sides). We linearize system (1.6), expanding  $\mathbf{F}(z)$  in a Taylor series in the vicinity of  $z^n$  (where  $n$  is the approximation number), and limit ourselves to the linear term

$$\frac{dz^{n+1}}{dx} = J(z^n)(z^{n+1} - z^n) + F(z^n), \quad (1.7)$$

where  $J(z^n)$  is a Jacobi matrix of partial derivatives of the right sides of system (1.6). Thus, in each approximation for  $z^{n+1}$  we have the linear problem of Eqs. (1.7), (1.3). To solve the latter we approximate system (1.7) by a finite difference scheme of second-order accuracy:

$$\frac{z_{i+1}^{n+1} - z_i^{n+1}}{h_i} = \frac{1}{2}[J(z_{i+1}^n)(z_{i+1}^{n+1} - z_{i+1}^n) + J(z_i^n)(z_i^{n+1} - z_i^n) + F(z_{i+1}^n) + F(z_i^n)]. \quad (1.8)$$

The system of two-point vector equations (1.8) together with condition (1.2) is solved by the matrix drive method [16]. This successive approximation method has quadratic convergence, and calculation of one variant requires two orders of magnitude less machine time than the method of establishing the steady-state solution.

**2. Calculation Results.** Calculations were performed for a gas mixture  $\text{CO}_2:\text{N}_2:\text{He} = 1:2:3$  for the following parameter values:  $L = 1$  cm,  $\gamma = 0.01$ , gas pressure  $p = 13.3$  kPa,  $N = 3.2 \cdot 10^{18}$   $\text{cm}^{-3}$ ,  $Q = 0-0.1$   $\text{C} \cdot \text{cm}^{-3} \cdot \text{sec}^{-1}$ ,  $\beta_e = 10^{-7}$   $\text{cm}^3 \cdot \text{sec}^{-1}$ ,  $K_d = 10^{-14}$   $\text{cm}^3 \cdot \text{sec}^{-1}$ ,  $\mu_+ = 18$   $\text{cm}^2 \cdot \text{V}^{-1} \cdot \text{sec}^{-1}$ ,  $\mu_- = 11$   $\text{cm}^2 \cdot \text{V}^{-1}$ . Data on ionization and attachment frequencies and electron mobility were taken from [17]. The results obtained for steady-state and nonsteady-state problems coincide, which indicates the reliability of both methods. Figure 1 depicts calculated discharge CVCs in the mixture studied for various intensities of the external ionization source. Curves 1-5 correspond to  $Q = 0, 0.001, 0.01, 0.03, 0.1$   $\text{C} \cdot \text{cm}^{-3} \cdot \text{sec}^{-1}$ . In comparison to the CVC of the discharge for the mixture  $\text{CO}_2:\text{N}_2:\text{He} = 1:1:8$  studied in [18], the CVC of the discharge in the mixture  $\text{CO}_2:\text{N}_2:\text{He} = 1:2:3$  is characterized by larger values of potential difference  $U$ . It is evident from Fig. 1 that the CVC of the dependent discharge has a segment with positive conductivity, corresponding to the regime in which the main contribution to ionization is made by the external source. The positive column in a discharge of this type has a homogeneous parameter distribution and is typical of both mixtures. Due to the low electric field in the positive column, shock ionization and electron attachment have only a weak effect on charged particle balance, the negative ion concentration is low, and the number of electrons and positive ions is defined by the expression  $\sqrt{Q/(\beta_e e)}$ .

Increase in potential difference across the discharge electrodes leads to intense changes in the positive column structure. The shaded area in Fig. 1 denotes a region of discharge instability, which appears in the calculations in the following manner. The current density  $j$ , obtained by solution of the nonsteady-state problem for a fixed potential difference  $U$ , oscillates in time, while upon solution of the steady-state problem the value of  $U$  defined for a given  $j$  oscillates from iteration to iteration; meanwhile the boundaries of the instability region as defined by each method coincide. We will note that in the instability region the plasma conductivity is close to zero (current saturation occurs). For each CVC the instability region is determined by two values of potential difference, dependent on the intensity of the external ionizer, which we shall denote by  $U_1$  and  $U_2$  ( $U_1 < U_2$ ).

The CVC segment below the instability region ( $U < U_1$ ) corresponds to a nonindependent discharge, in which at the boundary of the cathode layer and the positive column a static domain is formed [10]. Figure 2a shows the electric field intensity distribution and electron concentration (lines 1, 3), positive and negative ion concentrations (lines 2, 4) for a potential difference between the electrodes of 1.4 kV (the results presented in Figs. 2 and 3 were obtained for an external ionization source intensity  $Q = 0.01$   $\text{C} \cdot \text{cm}^{-3} \cdot \text{sec}^{-1}$ ). In the domain region the value of the electric field significantly exceeds that in the positive

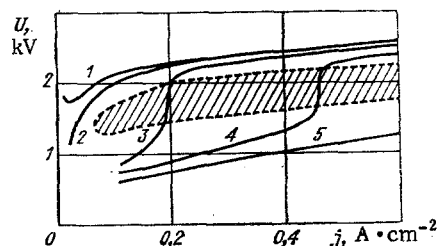


Fig. 1

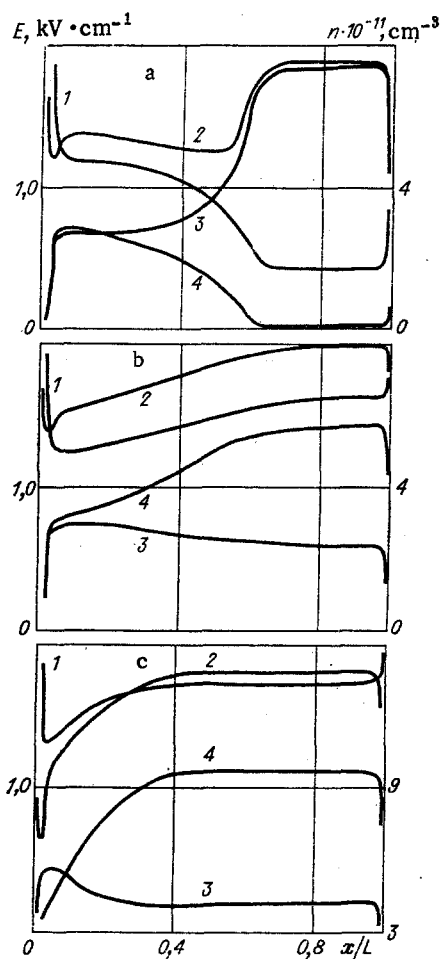


Fig. 2

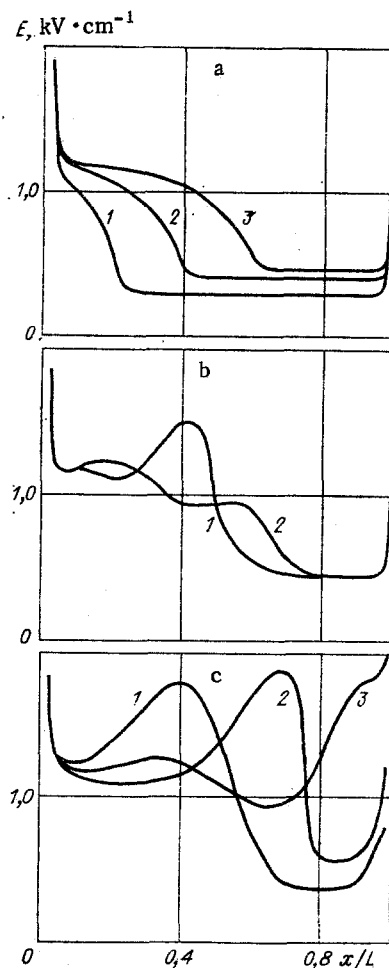


Fig. 3

column volume, loss of electrons occurring due to attachment, with the number of negative ions close to the number of electrons. In the remaining portion of the positive column ionization by the external source is compensated by recombination and  $n_e \gg n_-$ . The electric-field distributions for  $U = 1, 1.25, 1.4$  kV (curves 1-3) are shown in Fig. 3a. With increase in  $U$  the domain expands in the direction of the anode and the field intensity increases therein. Beginning at  $U_1 = 1.42$  kV increase in potential difference across the electrodes leads to instability of the discharge burn regime, at which point the current density begins to oscillate in time. These oscillations are related to the fact that the static domain, having reached its critical length  $l_*$ , will not expand further, but is torn away from the cathode layer and moves toward the anode. The calculations show that  $l_*$  increases with decrease in  $Q$ . Figure 3b shows electric field distributions for times  $t = 33, 37$   $\mu\text{sec}$  (curves 1, 2).

For an insignificant increase in voltage ( $U = 1.45$  kV) the freed domain damps out within the positive column volume, not reaching the anode (Fig. 3b), while for higher potential difference it reaches the anode and exits thereon (Fig. 3c,  $U = 1.85$  kV, curves 1-3 for  $t = 41, 45, 49$   $\mu\text{sec}$ ). Motion of the single domain corresponds to one oscillation period ( $\tau \approx 10$   $\mu\text{sec}$ ) of the current density. The velocity of the domain motion depends weakly on the applied potential and is of the order of  $10^3$  m/sec, while the domain dimensions increase with increase in  $U$ . The maximum electric field intensity in the moving domain is limited by the condition  $v_1(E/N) = v_{\alpha}(E/N)$  [10]. In a discharge corresponding to the upper limit of the instability region ( $U \lesssim U_2$ ), the domain occupies almost the entire volume of the positive column.

Upon transition through the value  $U_2 = 2.05$  kV the discharge again becomes stable. In this case the discharge positive column is inhomogeneous (Fig. 2b,  $U = 2.1$  kV) and its structure approaches that of an independent discharge (Fig. 2c,  $U = 2.4$  kV). The notation of Figs. 2b, c is the same as that of Fig. 2a. In such a discharge the electric field inten-

sity and ion concentration increase from cathode to anode, while the electron concentration falls, with  $n_+ > n_e$  over the entire positive column volume. The principles found agree qualitatively with results of an approximate analysis of the positive column [3] and the experiments of [2]. With increase in voltage across the electrodes the positive column of both independent and nonindependent discharges becomes more homogeneous (Fig. 2c).

A comparison of the attachment instability region of the present study with results obtained by linear stability analysis of a homogeneous positive column [4] is difficult, since because of inhomogeneity of the field distribution in the unstable discharge it is impossible to establish an unambiguous correspondence between the value of electric field intensity  $E$  at which the discharge is unstable in linear analysis, and the value of potential difference  $U$ , at which the discharge is unstable in numerical calculations. The value of  $Q$  for the lower instability limit of the discharge found in the present study is two orders of magnitude larger than that obtained by linear analysis. The calculations of the present study support the point noted in [9], that the size of the interelectrode distance affects the stability of the discharge: the larger  $L$ , the wider the discharge instability region with respect to  $Q$  (for example, at  $L = 2$  cm the discharge is unstable for  $Q = 0.001 \text{ C}\cdot\text{cm}^{-3}\cdot\text{sec}^{-1}$ ).

Thus, discharge current-voltage characteristics have been constructed for a  $\text{CO}_2\text{-N}_2\text{-He}$  mixture and the region of attachment instability has been determined. It has been shown that the structure of the positive column of a nonindependent discharge in electronegative gases changes from homogeneous distribution through an unstable state to an inhomogeneous parameter distribution depending on the applied voltage. It has been noted that the length of the discharge gap affects stability: the discharge instability region expands with increase in interelectrode distance in the direction of lower external ionization source intensities.

#### LITERATURE CITED

1. Yu. P. Raizer, *Fundamentals of Modern Physics of Gas Discharge Processes* [in Russian], Nauka, Moscow (1980).
2. E. P. Velikhov, V. S. Golubev, and S. V. Pashkin, "Glow discharge in a gas flow," *Usp. Fiz. Nauk*, 137, No. 1 (1982).
3. V. I. Blokhin and S. V. Pashkin, "A possible state of the positive column of a high voltage diffuse discharge in the presence of electronegative components," *Teplofiz. Vys. Temp.*, 17, No. 1 (1979).
4. D. H. Douglas-Hamilton and S. A. Mani, "Attachment instability in an externally ionized discharge," *J. Appl. Phys.*, 45, No. 10 (1974).
5. W. L. Nighan and W. J. Wiegand, "Influence of negative-ion processes on steady-state properties and striations in molecular gas discharges," *Phys. Rev.*, A10, No. 3 (1974).
6. A. D. Barkalov and G. G. Gladush, "Self-oscillating discharge regime in electronegative gases," *Zh. Tekh. Fiz.*, 49, No. 10 (1979).
7. A. D. Barkalov and G. G. Gladush, "Domain instability of a nonindependent discharge in electronegative gases. II. Theoretical analysis," *Teplofiz. Vys. Temp.*, 20, No. 2 (1982).
8. V. V. Breev, S. V. Dvurechenskii, and S. V. Pashkin, "Numerical study of nonsteady-state processes in the positive column of a high-voltage diffuse discharge. Analysis of the system of equations," *Teplofiz. Vys. Temp.*, 17, No. 1 (1979).
9. Yu. S. Akishev, S. V. Pashkin, et al., "On development of attachment instability in a confined plasma," *Teplofiz. Vys. Temp.*, 21, No. 2 (1983).
10. A. D. Barkalov and G. G. Gladush, "Domain instability of a nonindependent discharge in electronegative gases. I. Numerical calculation," *Teplofiz. Vys. Temp.*, 20, No. 1 (1982).
11. A. S. Kovalev, A. T. Rakhimov, and V. A. Feoktistov, "Establishment and decay of a non-independent discharge in an electronegative gas," *Fiz. Plazmy*, 8, No. 5 (1982).
12. V. V. Breev, S. V. Dvurechenskii, and S. V. Pashkin, "Numerical study of nonsteady-state processes in the positive column of a high-voltage diffuse discharge. Development and decay of the positive column plasma in air," *Teplofiz. Vys. Temp.*, 17, No. 2 (1979).
13. N. N. Kalitkin, *Numerical Methods* [in Russian], Nauka, Moscow (1972).
14. G. V. Gadiyak, A. G. Ponomarenko, and V. A. Shveigert, "Effect of preionization on development of an independent discharge in a gas," *Zh. Prikl. Mekh. Tekh. Fiz.*, No. 4 (1982).

15. R. E. Bellman and R. Kalaba, Quasilinearization and Nonlinear Boundary Problems [Russian translation], Mir, Moscow (1968).
16. A. A. Samarskii and E. S. Nikolaev, Methods for Solution of Grid Equations [in Russian], Nauka, Moscow (1978).
17. J. J. Lowke, A. V. Phelps, and B. W. Irwin, "Predicted electron transport coefficients and operating characteristics of CO<sub>2</sub>-N<sub>2</sub>-He laser mixtures," J. Appl. Phys., 44, No. 10 (1973).
18. R. S. Galeev, "Calculation of a steady-state glow discharge in a CO<sub>2</sub>-N<sub>2</sub>-He gas mixture," in: Mathematical Modeling in Physical Gas Dynamics [in Russian], Kazan. Inst., Kazan' (1985).

FORMATION OF AN ELECTRON BEAM-INDUCED SPARK DISCHARGE  
AT MINIMAL VOLTAGES

A. A. Aliverdiev, A. Z. Ėfendiev,  
and K. A. Ėfendiev

UDC 537.521+621.378

Entire monographs [1, 2] have already been dedicated to study of electron beam-induced spark discharges in gases. However, some features of the phenomenon remain insufficiently studied. In particular, it is not clear in what manner the discharge forms at minimal voltages. This question will be considered in the present study.

Studies were performed in technically pure nitrogen and air at atmospheric pressure. A beam of electrons with 1-MeV energy was injected into the gas chamber perpendicular to the electric field. The length of the discharge gap  $d = 0.4$  cm, with a discharge capacitance of  $0.25 \mu\text{F}$ , and brass electrode diameter of 2 cm. The lower traces of Fig. 1 show typical oscillograms of discharge current vs time in technically pure nitrogen (a) and air (b), while the upper traces are the electron beam pulse. Time scale is  $1 \mu\text{sec/division}$ . Values of electron flux intensity  $P_e$ , dependent discharge combustion voltage  $U_{dd}$ , electron concentration in the discharge gap  $n_e$  for the steady-state period of the independent discharge, combustion voltage of the quasisteady-state discharge  $U_{qd}$ , and spark discharge formation time  $t_f$ , measured from the moment of irradiation until appearance of the spark for an active external circuit resistance of  $7575 \Omega$  and electron beam pulse duration  $t_{ep}$  of  $0.5 \mu\text{sec}$  are presented in Table 1. Similar data for air at an active resistance of  $45,075 \Omega$  and electron pulse durations of  $0.5$  and  $1.5 \mu\text{sec}$  are given in Table 2. It is evident that the values of  $U_{dd}$ ,  $n_e$ ,  $U_{qd}$ , and  $t_f$  depend (for other conditions equal) on  $R$  and  $t_{ep}$ . This is controlled by the number of ionization acts and circuit time constant. Upon development of the independent discharge the voltage in the discharge circuit is redistributed. The value of  $n_e$  can be calculated from the condition  $n_e = I/Sq_e v_e$ , written in the form

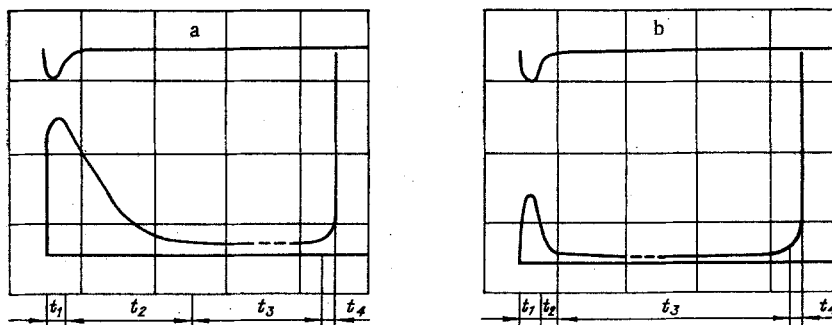


Fig. 1